Eur. Phys. J. Plus (2020) 135:544
https://doi.org/10.1140/epjp/s13360-020-00555-w

THE EUROPEAN PHYSICAL JOURNAL PLUS

Regular Article

Unidirectional flows of a Herschel–Bulkley fluid with pressure-dependent rheological moduli

Lorenzo Fusi[a]

Dipartimento di Matematica e Informatica "U.Dini", Universita degli Studi di Firenze, Viale Morgagni 67/a, 50134 Florence, Italy

Received: 20 November 2019 / Accepted: 21 June 2020

Abstract In this paper we study the planar channel flow of a Herschel–Bulkley fluid with pressure-dependent consistency index and yield stress. In particular we consider unidirectional flows in which the velocity is directed along the longitudinal direction of the channel. We show that unidirectional flows are possible only if the dependence on the pressure is linear, since in the nonlinear case secondary flow may appear. We determine constraints that ensure the existence of unyielded regions and constraints that guarantee that the flow does not come to a stop. Analytical solutions for the velocity field and the pressure are determined, and numerical examples that show the dependence on the physical parameters of the model are provided.

1 Introduction

In recent years problems regarding fluids in which the viscosity depends on the pressure have received a lot of attention among the scientific community. The classical Navier–Stokes incompressible model, in which the viscosity is constant, can describe the behavior of a large class of fluids in a large class of geometrical settings, but in some cases the assumption that the relation between the stress and the strain rate is a constant is simply not tenable. In the compressible Navier–Stokes model there are two material moduli (the bulk viscosity and the dynamic viscosity) that can depend on the density and, if one considers a nonisothermal setting, these moduli can also depend on the temperature. In [31] Stokes recognized that the viscosity of a linear fluid can depend on the pressure. In the compressible case the pressure is a function of the density defined through an equation of state, i.e., a constitutive equation. In the incompressible case the pressure is the Lagrange multiplier due to the incompressibility constraint and the stress cannot be written as an explicit expression of the symmetric part of the velocity gradient. Indeed[1]

$$\mathbf{T}^* = -p^*\mathbf{I} + 2\mu^*(p^*)\mathbf{D}^* = \left(\frac{1}{3}\,\mathrm{tr}\,\mathbf{T}^*\right)\mathbf{I} + 2\mu\left(\frac{1}{3}\,\mathrm{tr}\,\mathbf{T}^*\right)\mathbf{D}^* \tag{1}$$

[a] e-mail: lorenzo.fusi@unifi.it (corresponding author)
[1] Throughout the paper the starred variables denote dimensional quantities.

Published online: 04 July 2020

where

$$\mathbf{D}^* = \frac{1}{2}\left[\nabla^*\mathbf{v}^* + \nabla^*\mathbf{v}^{*T}\right], \tag{2}$$

$\mu^*(p^*)$ is the viscosity function and where p^* is the mean normal stress. In (1) we are tacitly assuming that $\operatorname{div}\mathbf{v}^* = \operatorname{tr}\mathbf{D}^* = 0$ (incompressibility constraint). We notice that while $\mathbf{T}^*$ is not given as an explicit expression of $\mathbf{D}^*$, the vice versa is true. In other words, in (1) we can express $\mathbf{D}^*$ as a function of $\mathbf{T}^*$. More generally the function μ^* may also depend on the invariants of $\mathbf{D}^*$. In this case we have a fully implicit relation between $\mathbf{D}^*$ and $\mathbf{T}^*$ of the form

$$\mathbf{g}^*(\mathbf{T}^*, \mathbf{D}^*) = 0.$$

When the function μ^* does not vary "too much" with the normal stress p^*, it can be approximated with a constant and Eq. (1) reduces to the classical incompressible Navier–Stokes model. A constitutive relation of the type (1) implies that the frictional forces exerted by adjacent layers of the fluid depend on the normal force that acts between the layers. This property is intuitive if one considers a solid sliding on another solid, so it is reasonable to assume that that this can happen also in a fluid. As an example we can think of an ocean or a deep lake, where adjacent layers near the bottom experience a larger frictional resistance than those in proximity of the surface.

Of course there are situations, such flows in pipes or channels, in which the dependence of viscosity on the pressure can be neglected. In those cases the classical linear model provides an excellent description of the flow and there is no need to take into account the dependence on the pressure. In other situations, such as flows entering extremely narrow domains or in elastohydrodynamic lubrication, the variation in the pressure can be so large that the viscosity is affected significantly and the dependence on the mean normal stress must be taken into account.

There is an abundant experimental literature that proves that the viscosity can depend on the pressure. A detailed discussion on the response of fluids and solids at very high pressure can be found in [3], while experimental works can be found in [16,21,22]. It has been proved that in some specific situations the dependence of viscosity on the pressure can also be exponential [1,32]. There are also many theoretical studies aimed at investigating flows with pressure-dependent viscosity. In [23] the authors have derived some analytical solutions for plane, round and annular Poiseuille flow for a Newtonian fluid in which the viscosity increases linearly with the pressure. In [18] Hron et al. have investigated some simple unidirectional flows for piezo-viscous fluids that are capable of shear thinning and shear thickening. More specifically they have considered the following extension of the constitutive Eq. (1)

$$\mathbf{T}^* = -p^*\mathbf{I} + 2\mu^*(p^*)\left|\mathbf{D}^*\right|^{\gamma-2}\mathbf{D}^*. \tag{3}$$

When $\gamma \in (-1, 2)$ the fluid can be shear thinning, while for $\gamma > 2$ the fluid can be shear thickening. When $\gamma = 2$ model (1) is recovered. In [30] Saccomandi et al. have investigated the lubrication flow of a piezo-viscous fluid with constitutive equation Eq. (1) down an incline in different flow regimes. In [24] Malek et al. have studied incompressible rate-type fluids with pressure- and shear rate-dependent material moduli. Some other particular steady and unsteady flows are studied in [5,28,29]. In recent years a remarkable attention has been brought to the case of visco-plastic fluids with pressure-dependent viscosity and yield stress. Analytical and numerical studies on visco-plastic fluids with pressure-dependent viscosity can be found in [4,7–15,20,26,27].

In this paper we investigate the unidirectional flow of a Herschel–Bulkley fluid with pressure-dependent moduli between parallel plates. Interestingly, this study has been carried

out in axisymmetric geometry (see [11,19]) but not in planar geometry. The scope of the present work is thus the extension of the results of [18] to the case of a visco-plastic fluid. The problem is not trivial, since now we have to determine the regions in which the fluid is unyielded (rigid plugs). Consistently with what found in [18] we show that unidirectional flows are possible only if the dependence of the rheological moduli on the pressure is linear. If this assumption is removed, then secondary flows appear and the flow is no longer unidirectional. We shall consider the flow driven by a prescribed flux with fixed boundaries, the flow between plates that are moving at constant speed and the flow of a layer of constant height with an imposed stress on the upper surface. In all these situations we derive analytical forms of the steady-state solutions for the velocity and for the pressure and we plot these solutions for different values of the physical parameters involved in the model. The paper is closed by a final section in which we discuss possible developments of the present work.

2 The mathematical model

We consider a Herschel–Bulkley fluid whose constitutive equation is given by $\mathbf{T}^* = -p^*\mathbf{I} + \mathbf{S}^*$ and where the deviatoric part $\mathbf{S}^*$ is expressed as

$$\begin{cases} \mathbf{S}^* = \left[2k^*(p^*)|\mathbf{D}^*|^{n-1} + \dfrac{\tau_o^*(p^*)}{|\mathbf{D}^*|}\right]\mathbf{D}^*, & |\mathbf{S}^*| \geqslant \tau_o^*, \\ \mathbf{D}^* = 0, & |\mathbf{S}^*|^* \geqslant \tau_o^*. \end{cases} \tag{4}$$

In Eq. (4) the quantities

$$|\mathbf{D}^*| = \sqrt{\frac{1}{2}\mathbf{D}^* : \mathbf{D}^*}, \qquad |\mathbf{S}^*| = \sqrt{\frac{1}{2}\mathbf{S}^* : \mathbf{S}^*}, \tag{5}$$

represent the norms of the tensors $\mathbf{D}^*$ and $\mathbf{S}^*$. The coefficient $n > 0$ (dimensionless) is the flow behavior index. When $n = 1$, Eq. (4) is the constitutive equation of a Bingham fluid with pressure-dependent parameters, see [12]. Differently from the classical Herschel–Bulkley model, here the consistency index k^* and the yield stress τ_o^* are supposed to be functions of the pressure p^*. In particular we assume that

$$k^*(p^*) = k_o^* f\Big(\alpha^*(p^* - p_o^*)\Big), \qquad [\alpha^*] = \mathrm{Pa}^{-1},$$
$$\tau_o^*(p^*) = Y^* g\Big(\beta^*(p^* - p_o^*)\Big), \qquad [\beta^*] = \mathrm{Pa}^{-1},$$

where f and g are positive nondecreasing functions such that $f(0) = g(0) = 1$. The characteristic values k_o^* and Y^* are the consistency index and yield stress at the reference pressure p_o^*.

The dependence of the viscosity on the pressure has been investigated since the pioneering work of Barus [2], where a exponential dependence was proposed. Other relations relating the viscosity to the pressure have also been proposed. In the reference [25] an exhaustive literature, both theoretical and experimental, on pressure-dependent fluids can be found. The pressure dependence of the yield stress in visco-plastic fluids (or visco-plastic material) is well known, especially when one considers granular materials that can be modeled as fluids, see [20]. In particular in [17] the dependence on the yield stress on the pressure and the temperature is investigated for some drilling fluids that can be modeled as Bingham or Herschel–Bulkley materials. In the isothermal regime it was proved that the dependence on the pressure can be safely assumed to be linear, see [17].

In the absence of body forces, the governing equations are

$$\begin{cases} \nabla^* \cdot \mathbf{v}^* = 0, & \{|\mathbf{S}^*| \leqslant \tau_o^*\} \cup \{|\mathbf{S}^*| \geqslant \tau_o^*\}, \\ \rho^* \dot{\mathbf{v}}^* = -\nabla^* p^* + \nabla^* \cdot \mathbf{S}^*, & \{|\mathbf{S}^*| \geqslant \tau_o^*\}, \\ \int\limits_{\Omega^*} \rho^* \dot{\mathbf{v}}^* d\mathbf{x}^* = \int\limits_{\partial\Omega^*} \mathbf{T}^* \mathbf{n}\, dA^*, & \{|\mathbf{S}^*| \leqslant \tau_o^*\}, \\ \mathbf{D}^* = 0, & \{|\mathbf{S}^*| \leqslant \tau_o^*\}. \end{cases} \tag{6}$$

where the superimposed dot stands for material time differentiation and where Ω^* represents any connected region in which the fluid is unyielded with outward unit normal $\mathbf{n}$. System (6) must be completed with appropriate initial and boundary conditions. Equation $(6)_1$ represent balance of mass in the whole domain, while $(6)_{2,3}$ represent balance of linear momentum of the yielded and unyielded phases, respectively. Equation $(6)_4$ comes from the assumption that the body is rigid in the unyielded domain. The momentum balance in the unyielded part is written in an integral form, since in Ω^* the stress is indeterminate, see [9]. The yield surface is defined through

$$|\mathbf{D}^*|\Big|_{\partial\Omega^*} = 0, \qquad \Longleftrightarrow \qquad |\mathbf{S}^*|\Big|_{\partial\Omega^*} = \tau_o^*(p^*)\Big|_{\partial\Omega^*}.$$

Finally, we assume that the stress is continuous across any yield surface. We consider three types of motion

1. Flow between parallel plates driven by a prescribed flux;
2. Flow between parallel plates moving at constant speed;
3. Flow of a layer of constant height with imposed stress on the upper surface.

In all cases the flow is assumed to be 2D and we write

$$\mathbf{v}^* = u^*(x^*, y^*, t^*)\mathbf{e}_1 + v^*(x^*, y^*, t^*)\mathbf{e}_2.$$

In case 1, assuming symmetry, we may define the unyielded phase as

$$\left\{|\mathbf{S}^*| \leqslant \tau_o^*\right\} = \left\{(x^*, y^*) : y^* \in [-\sigma^*, \sigma^*]\right\}, \tag{7}$$

and the yielded phase as

$$\left\{|\mathbf{S}^*| \geqslant \tau_o^*\right\} = \left\{(x^*, y^*) : \quad y^* \in [-H^*, -\sigma^*] \cup [\sigma^*, H^*]\right\}, \tag{8}$$

where $y^* = \pm\sigma^*(x^*, t^*)$ denote the yield surfaces and $2H^*$ is the distance between the plates. Moreover we impose no-slip on $y^* = \pm H^*$

$$\mathbf{v}^*\Big|_{\pm H^*} = 0,$$

and we impose the flux

$$Q^* = \int_{-H^*}^{H^*} u^*(x^*, y^*, t^*) \mathrm{d}y^*, \tag{9}$$

that does not depend on the longitudinal coordinate x^* because of incompressibility constraint. In case 2 we assume that the upper plate moves with velocity V^* while the lower plate is kept fixed. Hence

$$\mathbf{v}^*\Big|_{H^*} = U^*, \qquad \mathbf{v}^*\Big|_{-H^*} = 0,$$

and the flux is still given by (9). In case 3 we impose the normal and tangential stress on the upper surface

$$\begin{cases} \mathbf{T}^*\mathbf{e}_2 \cdot \mathbf{e}_2 = p^*_{\text{ext}}, \\ \mathbf{T}^*\mathbf{e}_2 \cdot \mathbf{e}_1 = \tau^*. \end{cases} \tag{10}$$

3 Nondimensional problem: unidirectional flows

The equations are nondimensionalized using the lengthscale H^*, the stress/pressure scale p^*_o, the velocity scale

$$U^*_o = H^* \left(\frac{p^*_o}{k^*_o}\right)^{\frac{1}{n}},$$

the timescale $H^* U^{*-1}_o$ and setting $p^* - p^*_o = p^*_o p$. We introduce the nondimensional coefficients

$$\alpha = \alpha^* p^*_o, \qquad \beta = \beta^* p^*_o,$$

together with the Bingham and Reynolds numbers

$$\mathsf{Bn} = \left(\frac{Y^* H^{*n}}{k^*_o U^{*n}_o}\right), \qquad \mathsf{Re} = \left(\frac{\rho^* H^{*2} p^{*\frac{2}{n}-1}_o}{k^{*\frac{2}{n}}_o}\right).$$

The stress tensor and the symmetric part of the velocity gradient become

$$\mathbf{S} = \left[2f(\alpha p)|\mathbf{D}|^{n-1} + \frac{\mathsf{Bn}\, g(\beta p)}{|\mathbf{D}|}\right]\mathbf{D}, \qquad \mathbf{D} = \frac{1}{2}\begin{bmatrix} 2u_x & (u_y + v_x) \\ (u_y + v_x) & 2v_y \end{bmatrix},$$

with norms

$$|\mathbf{S}| = 2f(\alpha p)|\mathbf{D}|^n + \mathsf{Bn}\, g(\beta p), \qquad |\mathbf{D}| = \sqrt{(u_x)^2 + \frac{1}{4}\left(u_y + v_x\right)^2}.$$

The governing equations in dimensionless form are

$$\begin{cases} \nabla \cdot \mathbf{v} = 0, & \{|\mathbf{S}| \leqslant \mathsf{Bn}\, g(\beta p)\} \cup \{|\mathbf{S}| \geqslant \mathsf{Bn}\, g(\beta p)\}, \\ \mathsf{Re}\, \dot{\mathbf{v}} = -\nabla p + \nabla \cdot \mathbf{S}, & \{|\mathbf{S}| \geqslant \mathsf{Bn}\, g(\beta p)\}, \\ \mathsf{Re} \int\limits_{\Omega} \dot{\mathbf{v}} d\mathbf{x} = \int\limits_{\partial\Omega} \mathbf{T}\mathbf{n}\, dA, & \{|\mathbf{S}| \leqslant \mathsf{Bn}\, g(\beta p)\}, \\ \nabla \mathbf{v} = 0, & \{|\mathbf{S}| \leqslant \mathsf{Bn}\, g(\beta p)\}. \end{cases} \tag{11}$$

The yield condition is

$$|\mathbf{D}|\Big|_{\partial\Omega} = 0, \qquad \Longleftrightarrow \qquad |\mathbf{S}|\Big|_{\partial\Omega} = \mathsf{Bn}\, g(\beta p)\Big|_{\partial\Omega},$$

In case the flux is prescribed, we rescale Q^* with $2H^*U^*_o$ so that

$$2q = \int_{-1}^{1} u(x, y, t)\mathrm{d}y. \tag{12}$$

We look for solutions of the type

$$\mathbf{v} = u(y)\mathbf{i}, \qquad p = p(x, y), \tag{13}$$

that is unidirectional flows. As proved in [18] for nonlinear piezo-viscous fluids the existence of unidirectional flows depends on the particular relation that links the viscosity/yield limit to the pressure (linear, exponential, etc.). Indeed, in general, one cannot assume the existence of a unidirectional flow like (13) when the rheology depends on the pressure, since this dependence may induce a secondary flow. Consistently with what found in [12,18] we shall see that a nontrivial unidirectional flow is possible when the consistency index and the yield stress are linear functions of the pressure.

4 Flow between parallel plates driven by a prescribed flux: case 1

When the flow is given by (13), we have

$$|\mathbf{D}| = \frac{1}{2}|u_y|, \qquad \mathbf{D} = \frac{1}{2}\begin{bmatrix} 0 & u_y \\ u_y & 0 \end{bmatrix}.$$

The mass balance is automatically satisfied and the normal stress components $S_{11} = S_{22} = 0$, while

$$S_{12} = \left[2^{(1-n)} f(\alpha p)|u_y|^n + \mathsf{Bn}\, g(\beta p)\right] \operatorname{sign}(u_y). \tag{14}$$

Equation $(11)_2$ reduces to

$$\begin{cases} p_x = \left(S_{12}\right)_y, \\ p_y = \left(S_{12}\right)_x, \end{cases} \tag{15}$$

while Eq. $(11)_3$ becomes

$$0 = \int_{\partial\Omega} \mathbf{T}\mathbf{n}\, dA, \tag{16}$$

where Ω represents the rigid plug. If one assumes for simplicity that the length of the channel is equal to its half amplitude ($L^* = H^*$), then following [9] and recalling that $S_{11} = 0$, Eq. (16) reduces to

$$\int_0^1 \left[\sigma_x p + S_{12}\right]_\sigma = (\sigma p)\Big|_0 - (\sigma p)\Big|_1. \tag{17}$$

where $(\sigma p)\Big|_i$ represents the force acting on the lateral surface of the core ($i = 0, 1$).

4.1 Pressure equation

From (15) it is clear that p satisfies the one-dimensional wave equation $p_{xx} = p_{yy}$. Exploiting D'Alembert formula we write

$$p(x, y) = m(x + y) + n(x - y)$$

Symmetry with respect to y implies that $p_y(x, 0) = 0$ so that

$$p(x, y) = m(x + y) + m(x - y).$$

Let us rewrite (14) as

$$S_{12} = F(p)J(y) + G(p). \tag{18}$$

From $(15)_2$

$$p_y = \Big[F_p(p)J(y) + G_p(p)\Big]p_x,$$

that is

$$\frac{m'(x+y) - m'(x-y)}{m'(x+y) + m'(x-y)} = J(y)F_p\Big(m(x+y) + m(x-y)\Big) + G_p\Big(m(x+y) + m(x-y)\Big).$$

After a little algebra we find

$$\frac{\left[\dfrac{m'(x+y) - m'(x-y)}{m'(x+y) + m'(x-y)} - G_p\Big(m(x+y) + m(x-y)\Big)\right]}{F_p\Big(m(x+y) + m(x-y)\Big)} = J(y). \tag{19}$$

Therefore the only F, G for which a unidirectional flow is allowed are the ones for which the left-hand side of (19) does not depend on x. If a choice of F, G does not satisfy (19), then a secondary flow appears in the channel. Establishing a criterion for selecting the F and G that produce a unidirectional flow is not easy, but we can use (19) to check whether a specific form of F and G can produce a unidirectional flow. When F and G are constant (classical Herschel–Bulkley model), we have $F_p = G_p = 0$ and

$$m'(x+y) = m'(x-y)$$

In this case

$$m(x) = Kx + C \tag{20}$$

and the pressure becomes

$$p(x) = Lx + R, \tag{21}$$

where L, C, Z, R are constants. Relation (21) represents the classical linear profile of the pressure for the one-dimensional unidirectional flow of a Herschel–Bulkley fluid in a channel. When F and G are linear in p, then F_p and G_p are constant

$$\frac{m'(x+y) - m'(x-y)}{m'(x+y) + m'(x-y)} = F_p I(y) + G_p = L(y). \tag{22}$$

Differentiating Eq. (22) with respect to x we find

$$\frac{m''(x+y)}{m'(x+y)} = \frac{m_{,,}(x-y)}{m'(x-y)} = const.$$

Therefore

$$m(z) = Ke^{Cz} + Z, \tag{23}$$

and p is given by

$$p(x, y) = Le^{Cx}\cosh(Cy) + R, \tag{24}$$

where L, C, Z, R are again constants.

4.2 Linear consistency index and yield stress

Suppose now that the consistency index and the yield stress are linear functions of the pressure, i.e.

$$f(\alpha p) = 1 + \alpha p, \qquad g(\beta p) = 1 + \beta p$$

We introduce

$$P = 1 + \alpha p.$$

The stress component S_{12} can be rewritten as

$$S_{12} = \frac{P}{\alpha} \underbrace{\left[2^{(1-n)}\alpha |u_y|^n + \phi\right] \operatorname{sign}(u_y)}_{=I(y)} + \underbrace{\frac{\mathsf{Bn}}{\alpha}(\alpha - \beta)\operatorname{sign}(u_y)}_{=const}, \tag{25}$$

where we have set

$$\phi = \mathsf{Bn}\,\beta > 0.$$

The momentum balance in the yielded phase becomes

$$\begin{cases} P_x = I_y P + I P_y \\ \\ P_y = I P_x. \end{cases} \tag{26}$$

Hence

$$\frac{P_x}{P} = \frac{I_y}{(1 - I^2)}, \qquad \frac{P_y}{P} = \frac{I I_y}{(1 - I^2)}, \tag{27}$$

and

$$\frac{P_x}{P} = \frac{I_y}{(1 - I^2)} = \left[\frac{1}{2}\ln\left(\frac{|I + 1|}{|I - 1|}\right)\right]_y = C_1(y),$$

where $C_1(y)$ is a function to be determined. Integrating the above we get

$$P(x, y) = \pm C_2(y) e^{C_1(y)x}. \tag{28}$$

From $(26)_2$ we find

$$P_y = \pm C_{2_y} e^{C_1 x} \pm C_{1_y} C_2 x e^{C_1 x} = \pm I C_2 C_1 e^{C_1 x},$$

implying that C_1 is a constant and

$$C_{2_y} - I C_2 C_1 = 0. \tag{29}$$

From $(27)_2$

$$\frac{P_y}{P} = \frac{\pm C_{2_y} e^{C_1 x}}{\pm C_2 e^{C_1 x}} = \frac{C_{2_y}}{C_2} = I C_1 = \frac{I I_y}{(1 - I^2)}.$$

Integration of the last equality with respect to y yields

$$C_1 y + K = \frac{1}{2}\ln\left(\frac{|I + 1|}{|I - 1|}\right),$$

or equivalently

$$|I + 1| = |I - 1| e^{2(C_1 y + K)}. \tag{30}$$

From the definition of I in (25) we see that

$$I(\pm\sigma) = \mp\phi, \tag{31}$$

because we expect $u_y > 0$ in $y < 0$ and $u_y < 0$ in $y > 0$. Inserting (31) into (30) we get

$$\left|\phi^2 - 1\right| = \left|\phi^2 - 1\right| e^{4K}, \tag{32}$$

implying $K = 0$. Therefore

$$I + 1 = \pm(I - 1)e^{2C_1 y},$$

and

$$I(y) = \frac{\pm e^{2C_1 y} - 1}{\pm e^{2C_1 y} + 1} = \left[2^{(1-n)}\alpha|u_y|^n + \phi\right]\mathrm{sign}(u_y). \tag{33}$$

The function $I(y)$ is odd in y. Evaluating (33) in $y = \sigma$ we find

$$I(\sigma) = \frac{\pm e^{2C_1\sigma} - 1}{\pm e^{2C_1\sigma} + 1} = -\phi. \tag{34}$$

It is easy to check that the existence of a positive σ that satisfies (34) is guaranteed if we take the positive sign before the exponential if $\phi \in (0, 1)$ and the negative sign if $\phi > 1$. If $\phi = 1$, the only solution is $\sigma = 0$. Therefore setting $\eta = \mathrm{sign}(1 - \phi)$ we may rewrite (34) as

$$I(\sigma) = \frac{\eta e^{2C_1\sigma} - 1}{\eta e^{2C_1\sigma} + 1} = -\phi, \tag{35}$$

which provides the location of the yield surface

$$\sigma = \frac{1}{2C_1}\ln\left(\frac{|1 - \phi|}{1 + \phi}\right). \tag{36}$$

Notice that, in order to have a positive σ, the coefficient C_1 must be negative. This constraint is due to the fact that we are assuming that the motion occurs from left to right (recall that we are assuming that $u_y < 0$ in $y > 0$ and $u_y > 0$ in $y < 0$). The function $I(y)$ becomes

$$I(y) = \frac{\eta e^{2C_1 y} - 1}{\eta e^{2C_1 y} + 1} = \tanh(C_1 y)^\eta = \left[2^{(1-n)}\alpha|u_y|^n + \phi\right]\mathrm{sign}(u_y). \tag{37}$$

Differentiating (37) w.r.t. y we find

$$I_y(y) = \frac{\eta\tanh(C_1 y)^{\eta-1}C_1}{\left[\cosh(C_1 y)\right]^2} = 2^{(1-n)}\alpha n|u_y|^{n-1}\left[\mathrm{sign}(u_y)\right]^2 u_{yy} \tag{38}$$

The r.h.s. of (38) must be negative in a right neighborhood of σ (indeed $u_{yy}(\sigma) < 0$ otherwise the plug is traveling with a velocity which is slower than the fluid that surrounds it), while the l.h.s. is negative only if $\eta = 1$. Therefore our model makes sense only if $\eta = 1$, i.e. $\phi \in (0, 1)$. In conclusion

$$\sigma = \frac{1}{2C_1}\ln\left(\frac{1 - \phi}{1 + \phi}\right), \qquad -\phi = \tanh(C_1\sigma). \tag{39}$$

Notice that the position of the yield surface is independent of α. The condition $\sigma \in (0, 1)$ is guaranteed by the inequality

$$-\infty < C_1 \leqslant \frac{1}{2}\ln\left(\frac{1 - \phi}{1 + \phi}\right) = \overline{C}_1 < 0 \tag{40}$$

We can now exploit (29) to determine the function $C_2(y)$. We have

$$\frac{C_{2_y}}{C_2} = \left[\ln(|C_2|)\right]_y = C_1\left[\frac{e^{2C_1 y} - 1}{e^{2C_1 y} + 1}\right] = C_1\tanh(C_1 y) = \left[\ln(\cosh(C_1 y))\right]_y$$

so that

$$\pm C_2(y) = L\cosh(C_1 y), \tag{41}$$

where L is a positive constant. We finally find that

$$P(x, y) = L\cosh(C_1 y)e^{C_1 x}, \tag{42}$$

and

$$p(x, y) = \frac{L\cosh(C_1 y)e^{C_1 x} - 1}{\alpha}. \tag{43}$$

On the plates $y = \pm 1$ we assume no-slip condition. From (37) and recalling that $\eta = 1$

$$|u_y| = 2^{(1-\frac{1}{n})}\alpha^{-1}\Big[\,\mathrm{sign}(u_y)\tanh(C_1 y) - \phi\Big]^{\frac{1}{n}}.$$

We introduce

$$\tilde{\alpha} = \alpha^{-1}2^{(1-\frac{1}{n})}, \tag{44}$$

so that

$$\pm u_y = \tilde{\alpha}\Big[\,\pm\tanh(C_1 y) - \phi\Big]^{\frac{1}{n}},$$

or equivalently

$$\pm u_y = \tilde{\alpha}\Big[\,\tanh(C_1\sigma) \pm \tanh(C_1 y)\Big]^{\frac{1}{n}},$$

where the positive sign has to be selected for $y < 0$, while the negative sign is for $y > 0$. Considering the upper half of the channel ($y > 0$) and integrating between $y \geqslant \sigma$ and 1 we find

$$u(y) = \int_y^1 \tilde{\alpha}\Big[\,\tanh(C_1\sigma) - \tanh(C_1\xi)\Big]^{\frac{1}{n}} d\xi,$$

where σ is given by $(39)_1$. Therefore in the yielded phase $[-1, -\sigma] \cup [\sigma, 1]$ the velocity is given by

$$u(y) = \int_{|y|}^1 \tilde{\alpha}\Big[\,\tanh(C_1\sigma) - \tanh(C_1|\xi|)\Big]^{\frac{1}{n}} d\xi \tag{45}$$

The velocity of the rigid plug is

$$u(\sigma) = \int_\sigma^1 \tilde{\alpha}\Big[\,\tanh(C_1\sigma) - \tanh(C_1\xi)\Big]^{\frac{1}{n}} d\xi. \tag{46}$$

Recalling (12) the nondimensional flux is

$$q = \int_0^1 u(y)\mathrm{d}y = \sigma u(\sigma) + \int_\sigma^1 u(y)\mathrm{d}y,$$

hence

$$q = \sigma\int_\sigma^1 \tilde{\alpha}\Big[\,\tanh(-C_1\xi) - \phi\Big]^{\frac{1}{n}} d\xi + \int_\sigma^1 \mathrm{d}y\int_y^1 \tilde{\alpha}\Big[\,\tanh(-C_1\xi) - \phi\Big]^{\frac{1}{n}} d\xi. \tag{47}$$

Equation (47) can be interpreted as the Buckingham equation of the Herschel–Bulkley model with pressure-dependent rheology. Such an equation can be used to determine the constant C_1 once $q > 0$ is prescribed. From (39) we observe that

$$\lim_{C_1 \to -\infty} \sigma = 0.$$

From (47) it is easy to check that

$$\lim_{C_1 \to -\infty} q = \int_0^1 \mathrm{d}y \int_y^1 \left\{ \tilde{\alpha} \Big[1 - \phi \Big]^{\frac{1}{n}} \right\} d\xi = \left[\frac{\alpha^n}{2} (1-\phi) \right]^{\frac{1}{n}} = q_\infty > 0,$$

$$\lim_{C_1 \to \overline{C}_1} q = 0,$$

and that

$$\frac{\partial q}{\partial C_1} = -\int_\sigma^1 \mathrm{d}y \int_y^1 \left\{ \frac{\tilde{\alpha}}{n} \Big[\tanh(-C_1\xi) - \phi \Big]^{\frac{1}{n}-1} \operatorname{sech}^2(C_1\xi)\xi \right\} d\xi < 0.$$

showing that q is a decreasing function of C_1. We conclude that whenever $q \in (0, q_\infty)$ there exists a unique $C_1 \in (-\infty, \overline{C}_1)$ such that (47) is satisfied, irrespectively of n. Once C_1 is determined, we can evaluate the pressure coefficient L using (17).

Remark 1 We observe that

$$S_{12}\Big|_\sigma = -\mathsf{Bn} - \phi p = -\mathsf{Bn}\Big(1 + \beta p\Big), \qquad \sigma_x = 0,$$

so that Eq. (17) becomes

$$\sigma = \frac{\mathsf{Bn}}{\Delta p} \left[1 + \beta \int_0^1 p \mathrm{d}x \right], \tag{48}$$

where $\Delta p = p|_0 - p|_1$. Therefore when $\mathsf{Bn} = 0$, we have $\sigma = 0$, as expected. When, on the other hand, $\beta = 0$ the position of the yield surface is the one of the classical Herschel–Bulkley models with constant parameters and with imposed flux. Notice also that Eq. (48) can be used to evaluate the constant L.

4.3 Numerical examples

In Figs. 1, 2 and 3 we plot the velocity profiles for various C_1, with increasing ϕ and with $n = 0.5$ (pseudoplastic or shear thinning). The increase in the coefficient $|C_1|$ (which is due to an increase in the flux q) implies an increase in the plug velocity and a reduction in the plug amplitude for each fixed value of $\phi > 0$ (that is for each fixed Bingham number). This result shows that if we keep increasing the flux (and hence the pressure gradient) in the fluid, we observe a reduction in the unyielded phase where the stress is below the yield limit. This is physically consistent, as the increase in the pressure gradient produces an increase in the overall stress within the fluid. We also notice that the increase in the coefficient ϕ for a fixed coefficient C_1 has the opposite effect. Indeed, if we increase the Bingham number for a fixed pressure gradient coefficient C_1, the amplitude of the plug gets larger and the velocity of the plug is reduced. Looking at Fig. 1 we observe that when $\phi = 0$, i.e., when the Bingham number is 0, the rigid plug is absent ($\sigma = 0$) and the profile is the one of a fluid with pressure-dependent viscosity (like the one studied in Section 3 of [18]).

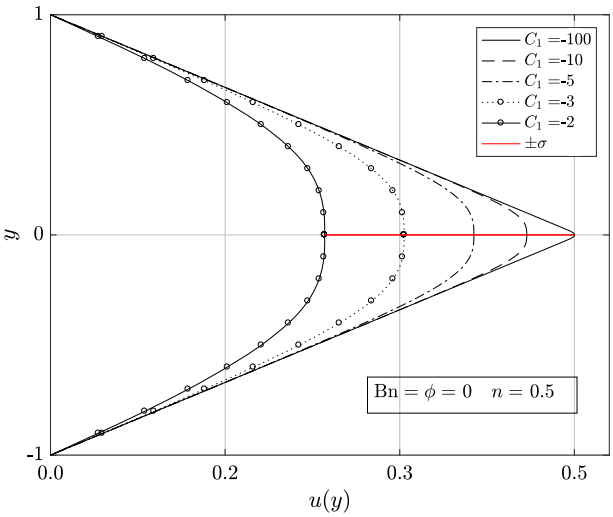

Fig. 1 Bn $= \phi = 0, n = 0.5$

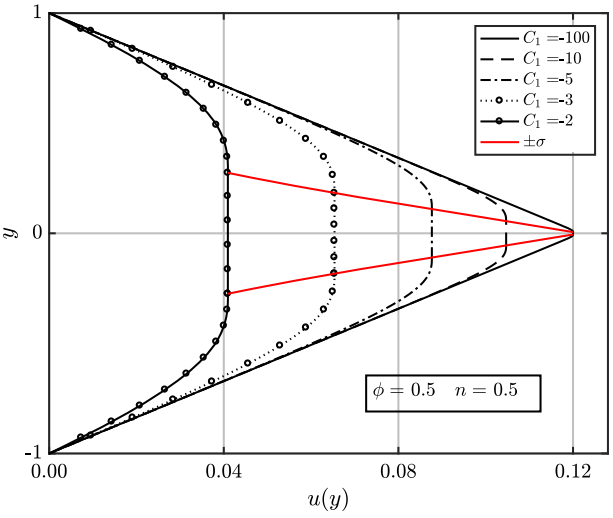

Fig. 2 $\phi = 0.5, n = 0.5$

The same behavior occurs when considering $n = 1$ (Bingham fluid with pressure-dependent rheology), as shown in Figs. 4, 5 and 6. We observe that the increase in the exponent n for the same values of ϕ and C_1 produces increase in the velocity of the plug but does not affect the amplitude of the unyielded plug, consistently with (39). In practice the dimension of the rigid core is independent of the particular nonlinearity of the stress–strain rate relation (linear, shear thickening or shear thinning).

Finally we take a look at the case $n = 1.5 > 1$ (dilatant or shear-thickening), see Figs. 7, 8 and 9.

Also in this case the increase in $|C_1|$ produces increase in the plug velocity and a reduction in the plug amplitude. And again, for fixed C_1 and ϕ the fluid shows a faster plug as n keeps

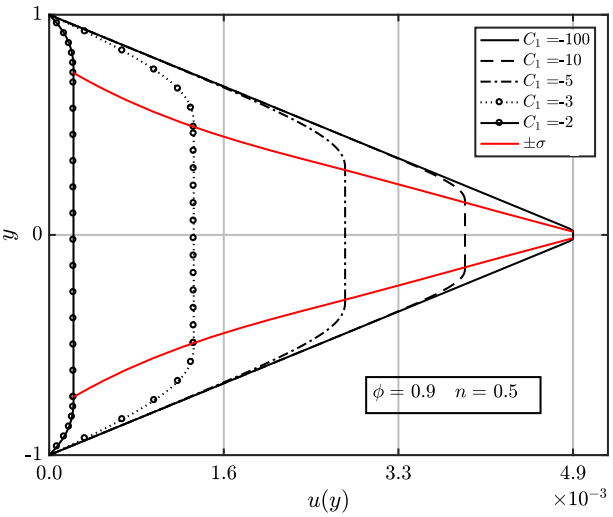

Fig. 3 $\phi = 0.9, n = 0.5$

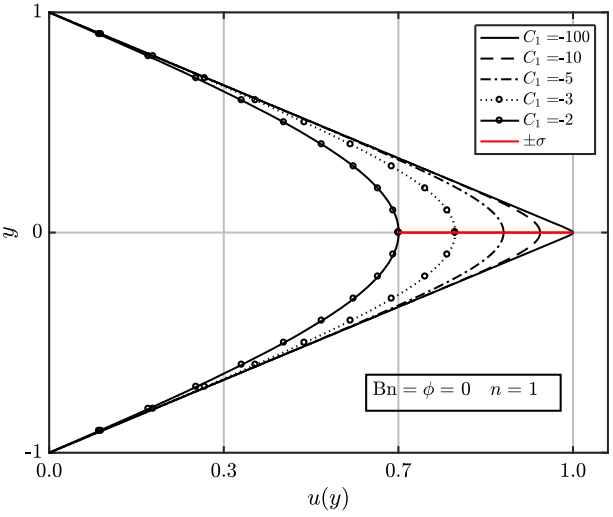

Fig. 4 $\mathrm{Bn} = \phi = 0, n = 1$

increasing. The pressure profiles (evaluated at the centerline of the channel and normalized with the constant L) are plotted in Figs. 10, 11. In all the plots in Figs. 1, 2, 3, 4, 5, 6, 7, 8, 9, 10 and 11 the coefficient α is normalized to one.

5 Flow between plates moving at constant speed: case 2

In this section we consider the flow between parallel plates in which the bottom plate is kept fixed while the upper plate moves with constant velocity $U > 0$. We retain the assumption that the rheological parameters depend linearly on the pressure and we consider again Eq. (25).

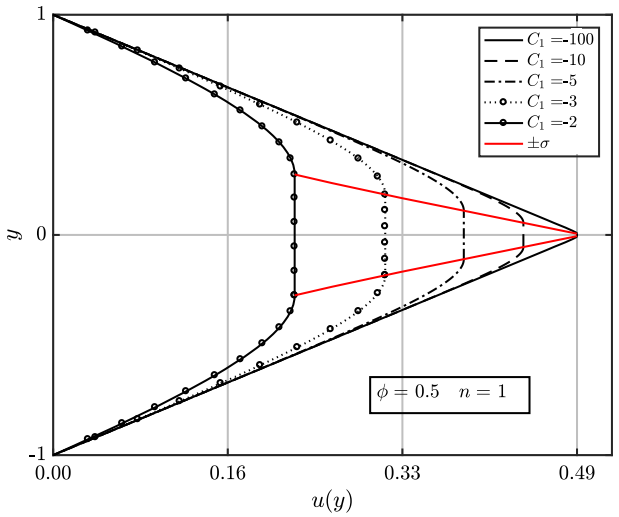

Fig. 5 $\phi = 0.5, n = 1$

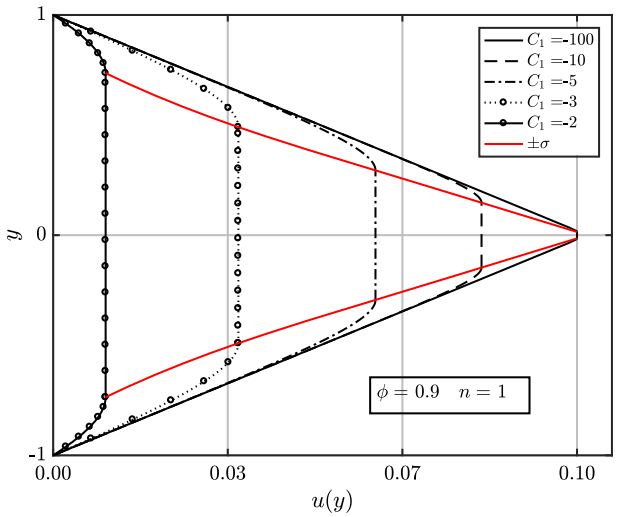

Fig. 6 $\phi = 0.9, n = 1$

It is reasonable to assume that the function $u_y > 0$ in the whole domain $[-1, 1]$, since the velocity grows from 0 to U in the layer. Hence

$$I(y) = 2^{(1-n)}\alpha\Big(u_y\Big)^n + \phi > 0.$$

From (30)

$$e^{2(C_1 y + K)} = \frac{|I+1|}{|I-1|} > 1, \qquad \forall\ I > 0.$$

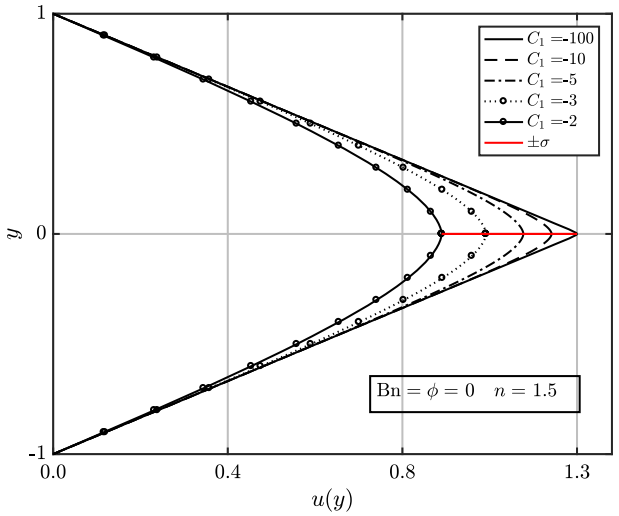

Fig. 7 Bn $= \phi = 0, n = 1.5$

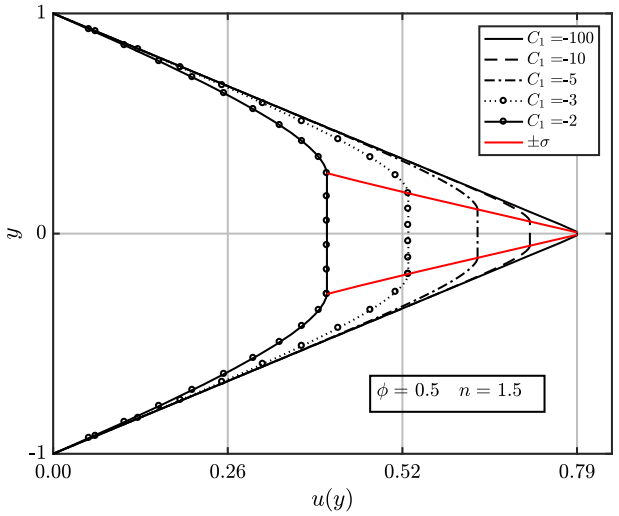

Fig. 8 $\phi = 0.5, n = 1.5$

implying that $C_1 y + K > 0$, i.e., $K > |C_1|$. On the yield surface $u_y(\sigma) = 0$, so that

$$I(\sigma) = \frac{\pm e^{2(C_1\sigma+K)} - 1}{\pm e^{2(C_1\sigma+K)} + 1} = \phi. \tag{49}$$

Again we must take the positive sign if $\phi \in (0, 1)$ and the negative sign for $\phi > 1$. Hence, recalling that $\eta = \text{sign}(1 - \phi)$ we get

$$\sigma = \frac{1}{C_1}\left[\frac{1}{2}\ln\left(\frac{1+\phi}{|1-\phi|}\right) - K\right]. \tag{50}$$

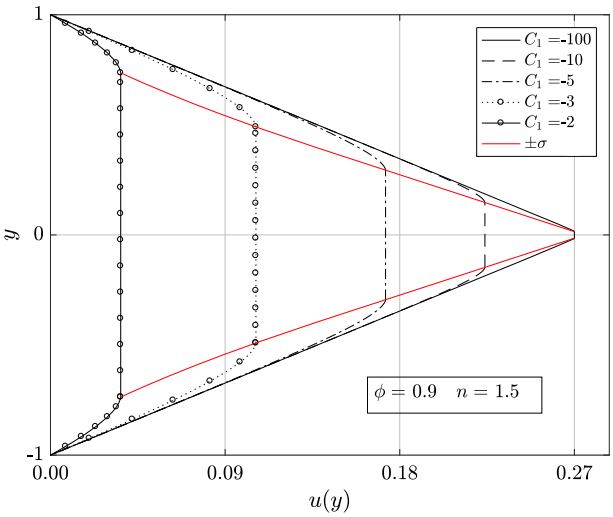

Fig. 9 $\phi = 0.9, n = 1.5$

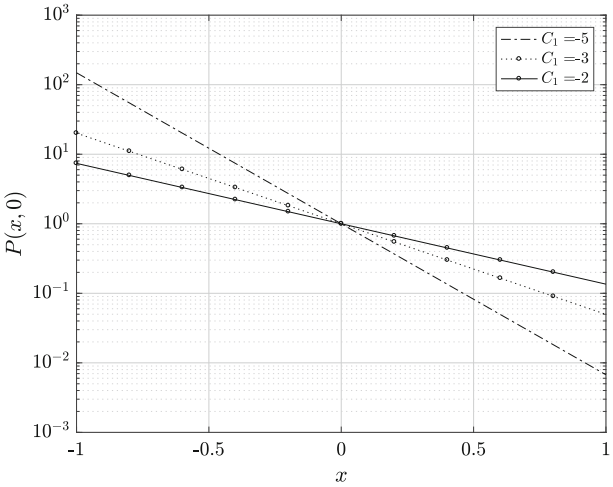

Fig. 10 Pressure $P(x, 0)$ for $C_1 = -2, -3, -5$

The yield surface is a function of C_1, K and ϕ, i.e. $\sigma = \sigma(C_1, K, \phi)$. Imposing $|\sigma| < 1$ and recalling that $K > |C_1|$ we find that K, C_1, ϕ must satisfy the following inequalities

$$\left| \frac{1}{2} \ln \left(\frac{1+\phi}{|1-\phi|} \right) - K \right| < |C_1| < K \tag{51}$$

Therefore the yield surface $\sigma \in (-1, 1)$ only if (51) is satisfied. In conclusion

$$\frac{\eta e^{2(C_1 y + K)} - 1}{\eta e^{2(C_1 y + K)} + 1} = 2^{(1-n)} \alpha \Big(u_y \Big)^n + \phi.$$

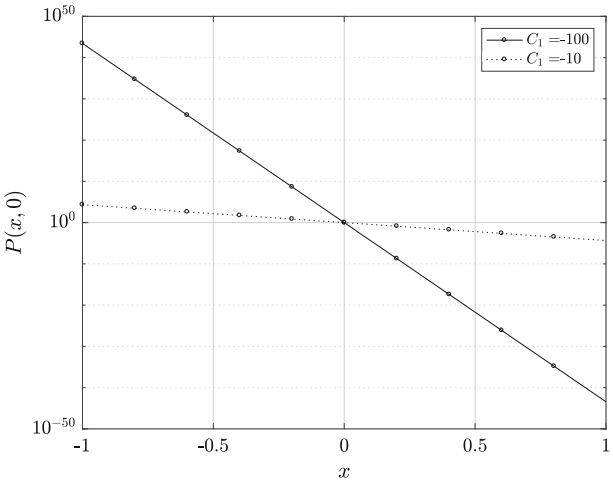

Fig. 11 Pressure $P(x, 0)$ for $C_1 = -10, -100$

that is

$$u_y = \tilde{\alpha}\left[\frac{\eta e^{2(C_1 y+K)}-1}{\eta e^{2(C_1 y+K)}+1} - \phi\right]^{\frac{1}{n}} = \tilde{\alpha}\left[\tanh(C_1 y + K)^{\eta} - \phi\right]^{\frac{1}{n}},$$

where $\tilde{\alpha}$ is still given by (44). Let us now evaluate u_y on the plates $y = \pm 1$. When (51) is satisfied, then

$$\text{(a)} \quad \eta C_1 > 0 \quad \begin{cases} \left[\tanh(C_1 y + K)^{\eta} - \phi\right]\Big|_{y=1} > 0 \\ \left[\tanh(C_1 y + K)^{\eta} - \phi\right]\Big|_{y=-1} < 0 \end{cases}$$

$$\text{(b)} \quad \eta C_1 < 0 \quad \begin{cases} \left[\tanh(C_1 y + K)^{\eta} - \phi\right]\Big|_{y=1} < 0 \\ \left[\tanh(C_1 y + K)^{\eta} - \phi\right]\Big|_{y=-1} > 0 \end{cases}$$

Therefore in case (a) the plug is adjacent to the lower plate while in case (b) is adjacent to the upper plate, as shown in the numerical examples. The constant K is determined imposing $u(1) = U$ and $u(-1) = 0$. We get

$$(\eta C_1 > 0) \qquad U = \int_{\sigma(C_1,K,\phi)}^{1} \tilde{\alpha}\left[\tanh(C_1 y + K)^{\eta} - \phi\right]^{\frac{1}{n}} \mathrm{d}y,$$

$$(\eta C_1 < 0) \qquad U = \int_{-1}^{\sigma(C_1,K,\phi)} \tilde{\alpha}\left[\tanh(C_1 y + K)^{\eta} - \phi\right]^{\frac{1}{n}} \mathrm{d}y.$$

where $\sigma = \sigma(C_1, K, \phi)$ is given by (50). In both cases $K = K(C_1, \phi)$ and if $K(C_1, \phi)$ satisfies (51), then $\sigma \in (-1, 1)$; otherwise the fluid is yielded everywhere in $(-1, 1)$ and the velocity gradient u_y is strictly positive everywhere in $(-1, 1)$. In conclusion we have that

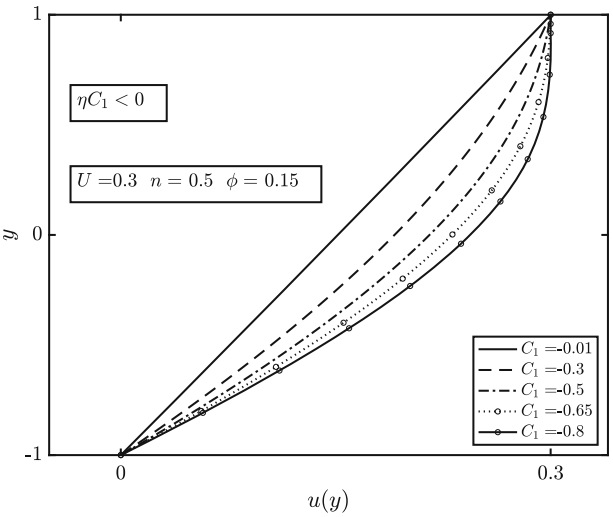

Fig. 12 $\eta C_1 < 0, n = 0.5$

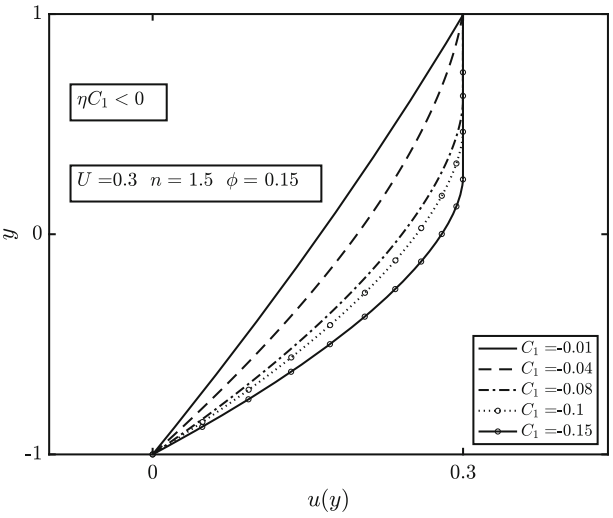

Fig. 13 $\eta C_1 < 0, n = 1.5$

$$(\eta C_1 > 0) \qquad u = \int_{\sigma(C_1,K,\phi)}^{y} \tilde{\alpha} \left[\tanh(C_1 z + K)^{\eta} - \phi\right]^{\frac{1}{n}} \mathrm{d}z, \tag{52}$$

$$(\eta C_1 < 0) \qquad u = U - \int_{y}^{\sigma(C_1,K,\phi)} \tilde{\alpha} \left[\tanh(C_1 z + K)^{\eta} - \phi\right]^{\frac{1}{n}} \mathrm{d}z. \tag{53}$$

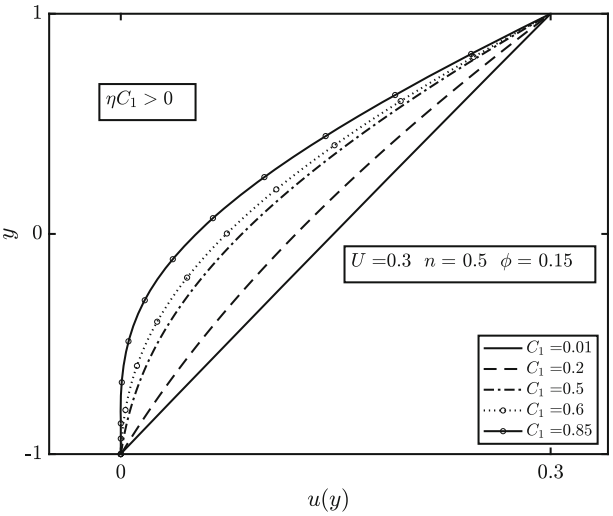

Fig. 14 $\eta C_1 > 0, n = 0.5$

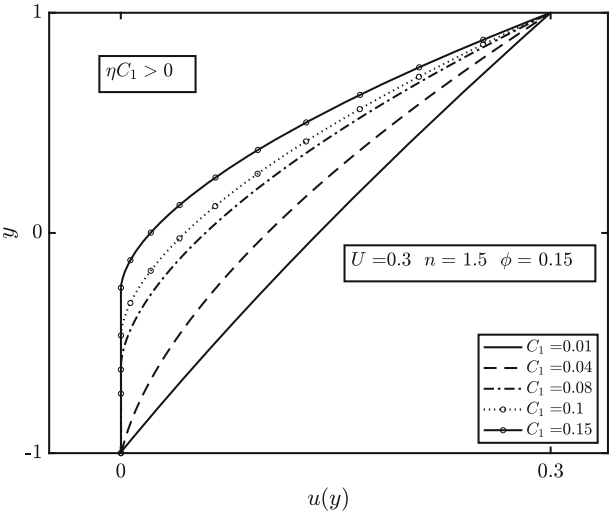

Fig. 15 $\eta C_1 > 0, n = 1.5$

5.1 Numerical examples

In this section we plot the velocity fields given by (52), (53) for different values of the parameters of the model. The velocity of the upper plate is set to $U = 0.3$, and the coefficient α is taken equal to one. In Figs. 12, 13 we display the velocity profiles in case $\eta C_1 < 0$, while in Figs. 14, 15 we show the case $\eta C_1 > 0$. For both cases we consider the shear-thinning behavior ($n = 0.5$) and the shear-thickening behavior ($n = 1.5$), taking $\phi = 0.15$. Since $\eta = \text{sign}(1 - \phi) = 1$, the sign of ηC_1 is changed by changing the sign of the pressure gradient coefficient C_1.

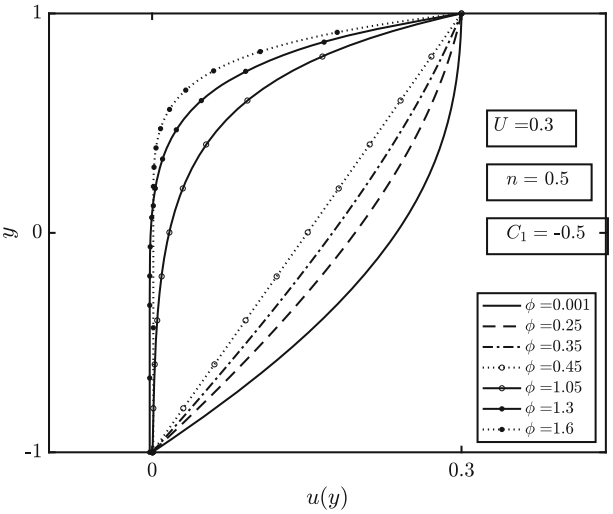

Fig. 16 Increasing ϕ

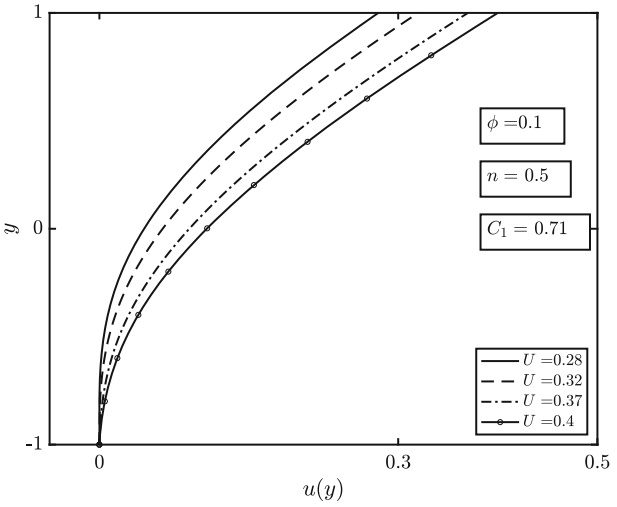

Fig. 17 Increasing V

We observe that the formation of an unyielded zone depends on the magnitude of the pressure gradient coefficient $|C_1|$. Indeed for small values of $|C_1|$ the fluid is yielded in the whole domain and $u_y > 0$ everywhere in $(-1, 1)$. As $|C_1|$ gets bigger the velocity near the upper/lower plate becomes uniform and the region where the stress is below the threshold (unyielded phase) starts to appear. Moreover we notice that for the dilatant fluid ($n > 1$) the pressure drop required to form the unyielded phase is smaller, i.e., the formation of the unyielded region occurs for values of $|C_1|$ that are smaller than in the pseudoplastic case ($n < 1$).

Finally in Figs. 16,17 we plot the velocity profiles for fixed values of $n = 0.5$, and C_1. In Fig. 16 we increase the values of ϕ (i.e., the Bingham number) observing that the concavity

of the solution changes as ϕ changes from being less than one to being larger than one. In Fig. 17 we see that the velocity is incremented as U is incremented, as expected.

6 Flow between plates with imposed stress on the upper surface: case 3

In this last case, from (10) we see that $S_{12} = \tau$ and $P = P_{\text{ext}}$ on $y = 1$, where τ and P_{ext} are the rescaled shear stress and external pressure $P = 1 + \alpha p$ at the top surface $y = 1$. Without loss of generality we may assume that $\tau > 0$. Recalling (25), (26) and (28) we see that

$$\left(IP\right)\Big|_1 - \left(IP\right)\Big|_y = C_1 \int_y^1 \pm C_2(\xi) e^{C_1 x} d\xi.$$

Recalling that

$$IP = \alpha S_{12} + \mathsf{Bn}\,(\beta - \alpha)\,\text{sign}\left(u_y\right),$$

we find

$$\alpha\tau + \mathsf{Bn}\,(\beta - \alpha)\,\text{sign}\left(u_y\right) = e^{C_1 x}\left[\pm C_2(y) I(y) + C_1 \int_y^1 \pm C_2(\xi) d\xi\right].$$

As a consequence $C_1 = 0$ and recalling (29) we also see that $\pm C_2$ is constant, i.e., $\pm C_2 = P_{\text{ext}}$. Therefore

$$I(y) = \left[2^{(1-n)}\alpha |u_y|^n + \phi\right]\text{sign}(u_y) = \frac{1}{P_{\text{ext}}}\left[\alpha\tau + \mathsf{Bn}\,(\beta - \alpha)\,\text{sign}\left(u_y\right)\right],$$

and

$$2^{(1-n)}\alpha |u_y|^n = \left[\frac{\alpha\tau\,\text{sign}\left(u_y\right) + \mathsf{Bn}\,(\beta - \alpha) - \phi P_{\text{ext}}}{P_{\text{ext}}}\right].$$

From (25) we see that $S_{12}(1) = \tau > 0$, hence $\text{sign}\left(u_y\right) = 1$, so that

$$u(y) = \tilde{\alpha}\left[\frac{\alpha\tau + \mathsf{Bn}\,(\beta - \alpha) - \phi P_{\text{ext}}}{P_{\text{ext}}}\right]^{\frac{1}{n}} (y + 1),$$

where we have exploited the condition $u(-1) = 0$. Therefore the motion is possible only if

$$\tau > \frac{\phi}{\alpha} + \frac{\mathsf{Bn}}{P_{\text{ext}}}\left(1 - \frac{\beta}{\alpha}\right),$$

and the velocity profile is a straight line. In this case the whole layer is yielded.

7 Conclusions and open problems

In this paper we have studied the unidirectional flow of a Herschel–Bulkley visco-plastic fluid with pressure-dependent rheology. We have extended the results of [18], proving that a unidirectional flow can exist only if the consistency index and the yield stress depend linearly on the pressure. This extension is not trivial since here, differently from [18], we are dealing with a free boundary problem due to the presence of the yield limit in the constitutive equation. Imposing mass and momentum balance we have found explicit expression for the velocity and for the pressure, showing that the latter depends on both coordinates x and y

differently from the constant case in which the dependence is only on x. We have found constraints on the parameters of the model that prevent the system from coming to a stop and other constraints that guarantee the existence of a truly unyielded region within the flow. We have considered three types of flow: (i) flow between parallel plates with a prescribed flux; (ii) flow between plates moving at constant speed; and (iii) flow of a layer with an imposed stress on the top free surface. For each flow we have plotted the velocity profiles for different values of the parameters involved in the model. The dependence on these parameters has been thoroughly discussed in the sections termed "numerical examples."

A natural continuation of this work, which we are currently developing, is the linear stability analysis of the stationary solutions determined in this paper. This problem is definitely of great interest since it can provide useful information on the effect of the dependence of the rheological moduli on the pressure. Linear stability in the classical case in which the viscosity and the yield stress are constant has been already studied (see [6]). The analysis for the nonconstant has not been carried out so far, so we do not know how the pressure dependence affect the evolution of small perturbations of the flow (linear stability analysis).

References

1. S. Bair, W.O. Winer, The high pressure high shear stress rheology of fluid liquid lubricants. J. Tribol. **114**, 1–13 (1992)
2. C. Barus, Isothermals, isopiestics and isometrics relative to viscosity. Am. J. Sci. **45**, 87–96 (1893)
3. P.W. Bridgman, *The Physics of High Pressure* (The MacMillan Company, New York, 1931)
4. Y. Damianou, G.C. Georgiou, On Poiseuille flows of a Bingham plastic with pressure-dependent rheological parameters. J. Non-Newton. Fluid Mech. **250**, 1–7 (2017)
5. M. Franta, J. Málek, K.R. Rajagopal, On steady flows of fluids with pressure- and shear-dependent viscosities. Proc. R. Soc. Lond. Ser. A **461**, 651–670 (2005)
6. I.A. Frigaard, S.D. Howison, I.J. Sobey, On the stability of Poiseuille flow of a Bingham fluid. J. Fluid Mech. **263**, 133–150 (1994)
7. L. Fusi, A. Farina, F. Rosso, Retrieving the Bingham model from a bi-viscous model: some explanatory remarks. Appl. Math. Lett. **27**, 11–14 (2014)
8. L. Fusi, A. Farina, F. Rosso, Mathematical models for fluids with pressure-dependent viscosity flowing in porous media. Int. J. Eng. Sci. **87**, 110–118 (2015)
9. L. Fusi, A. Farina, F. Rosso, S. Roscani, Pressure driven lubrication flow of a Bingham fluid in a channel: a novel approach. J. Nonnewton. Fluid Mech. **221**, 66–75 (2015)
10. L. Fusi, Unsteady non-isothermal flow of a Bingham fluid with non constant material moduli at low Reynolds number. Acta Mech. **229**, 193–210 (2018)
11. L. Fusi, F. Rosso, Creeping flow of a Herschel–Bulkley fluid with pressure-dependent material moduli. Eur. J. Appl. Math. **29**, 352–368 (2018)
12. L. Fusi, A. Farina, F. Rosso, Bingham flows with pressure-dependent rheological parameters. Int. J. Non-Linear Mech. **64**, 33–38 (2014)
13. L. Fusi, Non-isothermal flow of a Bingham fluid with pressure and temperature dependent viscosity. Meccanica **52**, 3577–3592 (2017)
14. L. Fusi, Channel flow of viscoplastic fluids with pressure-dependent rheological parameters. Phys. Fluids **30**, 073102 (2018)
15. L. Fusi, Lubrication flow of a generalized Casson fluid with pressure-dependent rheological parameters. J. Non-Newton. Fluid Mech. **274**, 104199 (2019)
16. E.M. Griest, W. Webb, R.W. Schiessler, Effect of pressure on viscosity of high hydrocarbons and their mixtures. J. Chem. Phys. **29**, 711–720 (1958)
17. J. Hermoso, F. Martinez-Boza, C. Gallegos, Combined effect of pressure and temperature on the viscous behaviour of all-oil drilling fluids. Oil Gas Sci. Technol. Rev. IFP Energ. Nouv. **69**, 1283–1296 (2014)
18. J. Hron, J. Malek, K.R. Rajagopal, Simple flows of fluids with pressure-dependent viscosity. Proc. R. Soc. Lond. (A) **457**, 1603–1622 (2001)
19. I. Ioannou, G.C. Georgiou, Axisymmetric Poiseuille flow of a Bingham plastic with rheological parameters varying linearly with pressure. J. Nonnewton. Fluid Mech. **259**, 16–22 (2018)

20. I.R. Ionescu, A. Mangeney, F. Bouchut, O. Roche, Viscoplastic modeling of granular column collapse with pressure-dependent rheology. J. Non-Newtonian Fluid Mech. **219**, 1–18 (2015)
21. K.L. Johnson, J.L. Tevaarwerk, Shear behaviour of elastohydrodynamic oil films. Proc. R. Soc. Lond. Ser. A **356**, 215–236 (1977)
22. K.L. Johnson, J.A. Greenwood, Thermal analysis of an Eyring fluid in elastohydrodynamic traction. Wear **61**, 355–374 (1980)
23. A. Kalogirou, S. Poyiadji, G.C. Georgiou, Incompressible Poiseuille flows of Newtonian liquids with a pressure-dependent viscosity. J. Non-Newton. Fluid Mech. **166**, 413–419 (2011)
24. J. Málek, K.R. Rajagopal, Incompressible rate type fluids with pressure and shear-rate dependent material moduli. Nonlin. Anal. Real World App. **8**, 156–164 (2007)
25. J. Málek, K.R. Rajagopal, *Mathematical Properties of the Solutions to the Equations Governing the Flow of Fluids with Pressure and Shear Rate Dependent Viscosities*, Handbook of Mathematical Fluid Dynamics (Elsevier, Amsterdam, 2007)
26. P. Panaseti, Y. Damianou, G.C. Georgiou, K.D. Housiadas, Pressure driven flow of a Herschel–Bulkley fluid with pressure-dependent rheological parameters. Phys. Fluids **30**, 030701 (2018)
27. P. Panaseti, G.C. Georgiou, I. Ioannou, Lubrication solution of the ow of a Herschel–Bulkley fluid with pressure-dependent rheological parameters in an asymmetric channel. Phys. Fluids **31**, 023106 (2019)
28. K.R. Rajagopal, G. Saccomandi, Unsteady exact solution for flows with pressure-dependent viscosities. Math. Proc. Roy. Irish Acad. **106A**, 115–130 (2006)
29. K.R. Rajagopal, K. Kannan, Flows of a fluid with pressure dependent viscosities between rotating parallel plates, in *New Trends in Mathematical Physics*, ed. by P. Fergola, et al. (World Scientific, Hackensack, 2004), pp. 172–183
30. G. Saccomandi, L. Vergori, Piezo-viscous flows over an inclined surface. Quart. App. Math. **4**, 747–763 (2010)
31. G.G. Stokes, On the theories of the internal friction of fluids in motion and of the equilibrium motion of elastic solids. Trans. Cambridge Phil. Soc. **8**, 287–305 (1845)
32. A.Z. Szeri, *Fluid Film Lubrication: Theory and Design* (Cambridge University Press, Cambridge, 1998)